



ELSEVIER

Available online at www.sciencedirect.com

ScienceDirect

Proceedings of the Combustion Institute 000 (2016) 1–8

Proceedings
of the
Combustion
Institutewww.elsevier.com/locate/proci

Structure of premixed H₂/O₂/Ar flames at 1–5 atm studied by molecular beam mass spectrometry and numerical simulation

D.A. Knyazkov^{a,b,*}, A.M. Dmitriev^{a,c}, T.A. Bolshova^a,
V.M. Shvartsberg^a, A.G. Shmakov^{a,c}, O.P. Korobeinichev^a

^a Voevodsky Institute of Chemical Kinetics and Combustion, Novosibirsk 630090, Russia

^b Far Eastern Federal University, Vladivostok 690950, Russia

^c Novosibirsk State University, Novosibirsk 630090, Russia

Received 3 December 2015; accepted 25 July 2016

Available online xxx

Abstract

A lack of available experimental data for spatial distributions of the species mole fractions in the flames of hydrogen at the pressures higher than atmospheric, which are required for developing and validating reliable kinetic models for hydrogen combustion, motivated this study. Stoichiometric laminar premixed H₂/O₂/Ar flames stabilized on flat burners at pressures 1, 3 and 5 atm were examined in this work by molecular beam mass spectrometry. Mole fraction profiles of all flame species (H₂, O₂, H₂O, H₂O₂, H, O, OH, HO₂) were measured. A decrease in the peak mole fractions of H, O, OH radicals and an increase in the peak mole fractions of HO₂ and H₂O₂ with pressure was observed. Two detailed kinetic mechanisms proposed recently by Konnov (2008) and Burke et al. (2012) for hydrogen combustion were validated against new experimental data reported in this work. Both mechanisms reproduced well the mole fraction profiles of H₂, O₂, H₂O and H, O, OH radicals in the flames. However, the mechanism of Burke et al. was found to be more adequate in predicting the mole fraction profiles of peroxy species in the flames. The observed changes in the flame structure with pressure were explained on the basis of a kinetic analysis of the model developed by Burke et al. The experimental data reported in this work can help in further development and improvement of the future kinetic models of hydrogen combustion at elevated pressures.

© 2016 by The Combustion Institute. Published by Elsevier Inc.

Keywords: Hydrogen; Molecular beam mass spectrometry; Burner-stabilized flame; Elevated pressure

1. Introduction

Combustion chemistry of hydrogen has been studied extensively for the last several decades, see e.g., [1–8] and references therein. However, despite these efforts, the interest for the mechanism of hydrogen combustion has not been exhausted

* Corresponding author at: Far Eastern Federal University, Vladivostok 690950, Russia. Fax: +7 383 3307350.

E-mail address: knyazkov@kinetics.nsc.ru
(D.A. Knyazkov).

<http://dx.doi.org/10.1016/j.proci.2016.07.109>

1540-7489 © 2016 by The Combustion Institute. Published by Elsevier Inc.

due to its particular importance for fundamental science and for practical applications. Validation of the proposed chemical kinetic mechanisms for combustion of fuels, including hydrogen, against the experimental mole fraction profiles of different species in flames (flame structure) is a key step in getting insight into the combustion kinetics.

In this regard, many studies have been focused on the measurements of species mole fractions in one-dimensional premixed hydrogen flames [9–18]. These data were obtained for the flames stabilized at low- and atmospheric-pressure conditions. The experimental data on the chemical speciation in the flames of hydrogen at elevated pressures (>1 atm) are extremely scarce. To our knowledge, only Paletskii et al. [16] measured the mole fraction of hydrogen, oxygen and water in flat burner-stabilized $\text{H}_2/\text{O}_2/\text{Ar}$ flame at the pressure of 10 atm using molecular beam mass spectrometry (MBMS). However, the mole fractions of major flame intermediates, which play the key role in hydrogen combustion were not measured in Paletskii et al. [16].

It is evident that detailed reaction mechanisms, tested only for the atmospheric or low pressure conditions, cannot be securely applied to description of processes proceeding at higher pressures. To develop reliable reaction mechanisms, the available experimental database, in particular, the database for spatial distributions of the species mole fractions in flames, should be expanded to the area of higher pressures, and the mechanisms should be validated against this database.

Thus, the abovementioned concerns motivated us to study premixed laminar burner-stabilized flames of hydrogen at 1, 3 and 5 atm using molecular beam mass spectrometry, which was applied recently to studying the structure of premixed methane flames in this range of pressures [19]. In this work, we report our MBMS measurement data on mole fraction profiles of all 8 species (H_2 , O_2 , H_2O , H , O , OH , HO_2 , H_2O_2) in the flame of stoichiometric $\text{H}_2/\text{O}_2/\text{Ar}$ mixture. Our goal was to provide experimental evidence of how the increase in pressure affects the species mole fractions in the flame. In this work, we used our data for validating recently updated detailed reaction mechanisms for hydrogen combustion proposed in the literature [5,6] and performed kinetic analysis of the mechanisms in order to explain the observed tendencies.

2. Experimental and modeling approaches

The flames of hydrogen/oxygen/argon mixtures were examined at the pressures of 1, 3 and 5 atm using a quadrupole mass spectrometer with a molecular beam sampling system and with ionization by electron impact. Although the experimental setup and procedures for studying the flames at elevated

pressures have been described thoroughly in our recent work [19], some specific details are given below.

The atmospheric-pressure flame was stabilized on a burner with a perforated matrix 16 mm in diameter, whereas at elevated pressures the burner with a porous matrix 6 mm in diameter was used. The latter was mounted in a high-pressure chamber, which was pressurized with nitrogen for the time of the experiment. The chamber was connected to a sampling probe flange of the MBMS setup. The temperature of the burners was kept at 333 K by circulation of thermostated water. Three stoichiometric flames of similar molar composition ($\text{H}_2/\text{O}_2/\text{Ar}=13.33/6.67/80\%$) were investigated at the pressures of 1, 3 and 5 atm. Linear velocities of the fresh mixtures at the burner surface (at 333 K) for the indicated pressures were 44.9, 39.9 and 23.9 cm/s, respectively. These values were chosen so that the flames were stable under particular conditions. In choosing the flame conditions, we added trace amounts of methane to the fresh mixtures to visualize the flames and ensure visually their flatness and stability.

Flame sampling was performed using a quartz conic probe with the opening angle of 40° , 18 mm height and the orifice diameter of 40 microns. The wall near the probe tip was 80 microns thick, and, getting closer to the base of the probe, its thickness increased gradually to be 2 mm at the probe base. A molecular beam was formed using a stainless-steel skimmer. Its tip was located 18 mm from the probe tip. The sample entered a collimator and the ionization chamber, where ionization of the gas occurred. The stage between the skimmer and the collimator was equipped with a modulator of the molecular beam. The use of the beam modulator allowed us to discriminate the beam signal from the signal of background species and therefore to eliminate possible dependence of the signal on the background pressure in the ionization area.

The mass spectrometer was equipped with an improved ion source with narrow spread of electron energies (± 0.25 eV), which corresponds to the basis width of the electron energy distribution function (thermal scattering) [20]. This allowed operation at low ionization energies which are close to the ionization potentials of the flame species. Electron energies were selected for each species analyzed, so as to obtain a fairly high signal-to-noise ratio, without interferences from fragmentation of other species.

The energies of ionizing electrons in the measurements of intensities of corresponding mass peaks were as follows: 16.65 eV for H , H_2 , O , OH , HO_2 , and 14.35 eV for H_2O , O_2 , and H_2O_2 . It should be noted that a typical mass spectrum of molecular oxygen with natural abundance of its isotopes (at least at ionizing electron energies below 18 eV) consists of three peaks: 32, 33 and 34, corresponding to $\text{O}^{16}\text{O}^{16}$ (major peak, $\approx 99.76\%$),

$\text{O}^{16}\text{O}^{17}$ ($\approx 0.04\%$) and $\text{O}^{16}\text{O}^{18}$ ($\approx 0.2\%$). Therefore, the signal intensities of the mass peaks corresponding to HO_2 and H_2O_2 ($m/z=33$ and 34 , respectively) in flames were corrected for contribution of oxygen molecules containing O^{17} and O^{18} isotopes.

According to literature data, appearance energy for fragment ions (HO_2^+ and OH^+) produced by electron impact ionization of H_2O_2 is about 15.35 eV [21], which is lower than the energy of ionizing electrons used in our work for OH and HO_2 measurements (16.65 eV). However, our measurements showed that the contributions of the fragmented ions from H_2O_2 to mass peaks 17 and 33 were negligible at the energy of 16.65 eV.

The mole fractions of the reactants (H_2 , O_2) and major stable species (H_2O , H_2O_2) were determined using the calibration coefficients (relative to argon) derived from direct calibration experiments with gas mixtures of known composition. The saturated $\text{H}_2\text{O}_2/\text{H}_2\text{O}/\text{Ar}$ mixture was prepared by passing of a flow of argon through a thermostated bubbler containing a solution of 35% wt. H_2O_2 , with the remainder being water. Mole fractions of H_2O_2 and H_2O vapors in the calibration mixture were determined using the values for the vapor pressure of hydrogen peroxide and water above the solution at a given temperature, similarly to what was done by Aul et al. [22].

Calibration coefficients for the flame radicals (H, O, OH and HO_2) were determined by applying a relative ionization cross-section method described by Cool et al. [23] and used in our previous work [19]. The idea of this method consists in the following. The calibration coefficient (S) links the signal intensity (I) with the mole fraction (X) for each species at a given temperature and pressure by a simple relation: $I = SX$. S is proportional to $\sigma(E)$, the ionization cross-section at electron energy E . Thus, the unknown calibration coefficient for an intermediate species is related to the known calibration coefficient for the nearest stable species by the following expression: $S_i = S_s \cdot [\sigma_i(E_i)/\sigma_s(E_s)]$, where index i corresponds to intermediate species, and index s corresponds to the nearest species with the known calibration coefficient. The electron ionization cross sections at a given electron energy for H, O and HO_2 were calculated using the NIST Electron Impact Cross Section Database [24], and for OH they were taken from [25]. The calibration coefficients for H, O and OH were also derived using an alternative method based on partial equilibrium by three “fast” reactions in the post-flame zone of the flames: $\text{H}_2 + \text{OH} \leftrightarrow \text{H}_2\text{O} + \text{H}$, $\text{H}_2 + \text{O} \leftrightarrow \text{H} + \text{OH}$, and $\text{O}_2 + \text{H} \leftrightarrow \text{OH} + \text{O}$, as done previously [18]. Good agreement between the calibration coefficients obtained with these two methods for H, O and OH was achieved.

The uncertainty of determining absolute mole fractions of the flame reactants and stable species (H_2 , O_2 , H_2O and H_2O_2) was estimated to be

$\pm 20\%$ of the maximum mole fraction values. This inaccuracy was mainly due to the errors in the measurements of the mass peak intensities and uncertainties in calibration. Absolute mole fractions of H, OH, O and HO_2 radicals were determined to be within a factor of about 2. This uncertainty was evaluated taking into account the following sources of errors: uncertainty in the measurement of mass peak intensities, and uncertainty in ionization cross section due to the electron energy spread.

To account for the cooling effect of the probe on the flame, we measured the temperature in the vicinity (slightly upstream) of the probe orifice for each HAB to obtain a perturbed temperature profile. This profile was used then as the input data for the flame structure calculations using PREMIX code [26]. Details of temperature measurements and PREMIX calculations will be given below.

The diameter of the probe orifice is the key parameter determining the quality of the experimental data, see, e.g., [27,28]. In this work we used the sampling probe with the orifice $40 \mu\text{m}$ in diameter as in our recent work [19], in which we studied premixed methane flames under similar conditions (at 1–5 atm). It was shown [19] that the use of such a probe provided quite reasonable spatial distributions of species mole fractions in the flames.

The temperature profiles in all the flames were measured using a Pt-(Pt+10% Rh) thermocouple located ~ 0.05 mm from the tip of the sampling probe in high-pressure flames and 0.2 mm from the probe tip in atmospheric-pressure flame. The thermocouple was welded from wires 0.02 mm in diameter covered with a thin layer of SiO_2 to prevent catalytic effects on its surface. The resulting thermocouple had a diameter of 0.03 mm. The temperature values measured with the thermocouple were corrected for radiative heat losses, as described in Shaddix [29]. The measurements of the temperature profiles were repeated several times. The maximum spread in the measured values of the temperature was up to ± 40 K. Therefore, this spread was considered as the temperature measurement uncertainty. Meanwhile, we are aware of the fact that the actual uncertainty of temperature measurements in the flame zone can be greater for the flames stabilized at 3 and 5 atm than for atmospheric-pressure flame due to greater temperature gradients. According to our previous findings [19], for the flames at 3 and 5 atm the experimental error limit at the heights above burner lower than ~ 0.2 mm can reach ± 150 K.

The mole fraction profiles of the flame species were simulated, using the PREMIX code from the CHEMKIN II collection of codes [26]. Two detailed chemical kinetic mechanisms proposed by Konnov [5] and Burke et al [6] were employed for modeling in this work. Both these mechanisms were validated by their authors against numerous experimental data. In particular, the

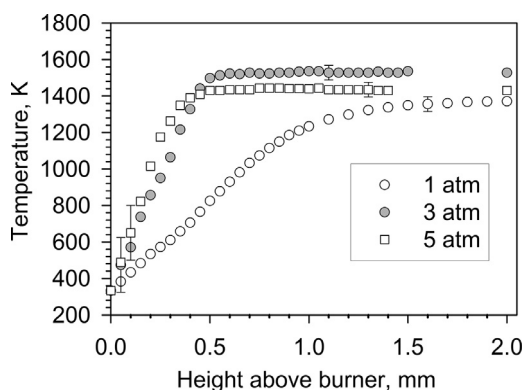


Fig. 1. Temperature profiles in premixed laminar stoichiometric $\text{H}_2/\text{O}_2/\text{Ar}$ flames at pressures 1, 3 and 5 atm.

Konnov model predicted adequately ignition, oxidation, flame burning velocities, and flame structure of hydrogen-oxygen-inert mixtures [5]. Burke et al. [6] reported that the predictions using their model adequately reproduced previous validation targets and showed substantially improved agreement against recent high-pressure flame speed and shock tube speciation measurements. The thermodynamic and transport properties provided with each mechanism by the authors were used. The calculations were performed with the measured temperature profiles, which were smoothed, as input data using the TGIV keyword. The PREMIX input files in CHEMKIN format used for the calculations are provided in the Supplemental Material (premix_1atm.inp, premix_3atm.inp, premix_5atm.inp).

3. Results and discussions

3.1. The structure of $\text{H}_2/\text{O}_2/\text{Ar}$ flames at atmospheric and elevated pressures

The experimental data represented below in Figs. 1–4 are provided in tabular form in the Supplemental Material (Experimental data.xls). The temperature profiles measured in the flames at atmospheric and elevated pressures are plotted in Fig. 1. As seen, the width of the flame zone largely decreases as the pressure increases from 1 to 3 atm, as expected: at the pressure of 1 atm, it is about 1.2 mm, while at 3 atm it is ~ 0.5 mm. Further increase in pressure from 3 to 5 atm results in a slight decrease in the width of the flame zone (from ~ 0.5 to ~ 0.4 mm). The values of the post-flame temperatures are determined essentially by the heat losses to the burner and do not depend on completeness of combustion. In Fig. 2, experimental mole fraction profiles of H_2 , O_2 and H_2O at 1, 3 and 5 atm are compared with those calculated using two re-

action mechanisms. As can be seen, although the mechanisms give slightly different predictions, they provide in general a good fit to these experimental data.

Measured and calculated mole fraction profiles of the chain carriers, i.e., H, O and OH radicals, are shown in Fig. 3. In view of the fact that the accuracy of determining absolute mole fractions of the radicals is fairly low (within a factor of 2 or even probably higher) one may state that the agreement between the experimental data and modeling results for all pressures in general is quite good. It should be noted that the mechanism of Burke et al. yields lower peak mole fractions of the radicals than Konnov mechanism. However, due to the abovementioned uncertainties, it is difficult to say, based on our data, which of them is better in predicting the mole fractions of the chain carriers. The pressure dependence of the peak mole fractions of the radicals will be discussed in the next section.

Comparisons of the measured and calculated mole fraction profiles of HO_2 radicals and hydrogen peroxide are shown in Fig. 4. The first thing to note in the diagrams is that the models predict maximums of the mole fractions of these species to be closer to the burner than those of H, O and OH radicals (see Fig. 3 to compare). This is due to the fact that formation of the peroxy species proceeds basically at low temperatures. Experimental data confirm this fact. However, as is seen, the peaks of the profiles were resolved clearly only for the flame at 1 atm due to the fact that the flame zone is significantly wider than those at elevated pressures. In addition, the absolute mole fractions of these species are very low ($\sim 10^{-4}$), which also could affect their measurement accuracy. Nevertheless, one can conclude from the comparisons of the measurement and calculation results that, in general, the predictions of the mechanism of Burke et al. are in better agreement with the experimental data for the peroxy species than those of the Konnov mechanism. Moreover, as is seen, the profiles calculated with the Konnov mechanism differ essentially from those with the Burke et al. mechanism: HO_2 peak mole fractions are much closer to the burner, and H_2O_2 profiles have two maximums. The experimental data for H_2O_2 , at least for atmospheric-pressure flame, definitely show a single peak, as well as the predictions of the Burke et al. mechanism.

Summarizing the results of the comparisons of the measurement data and calculation results using two detailed mechanisms from the literature, we come to the following conclusions: (1) both models are good in predicting H, O and OH mole fractions at the pressures considered; (2) the Burke et al. model is more adequate in reproducing the mole fraction profiles of peroxy species than the Konnov model. Therefore, in the following section the

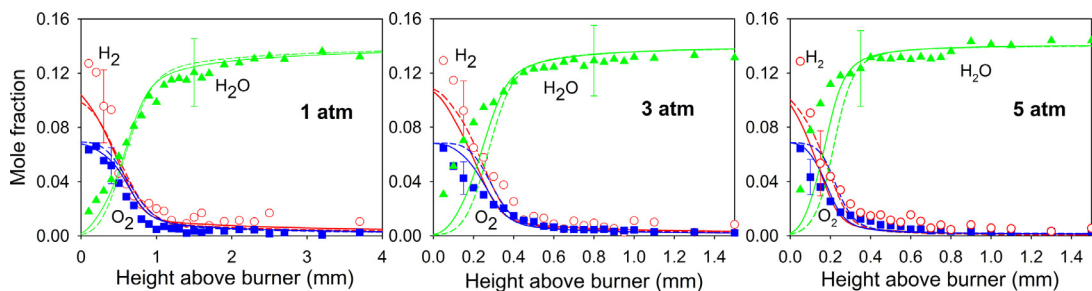


Fig. 2. Mole fraction profiles of H_2 , O_2 and H_2O in premixed laminar stoichiometric $\text{H}_2/\text{O}_2/\text{Ar}$ flames at pressures 1, 3 and 5 atm. Symbols: experimental data, lines: modeling (solid line: Konnov mechanism; dashed line: Burke et al. mechanism).

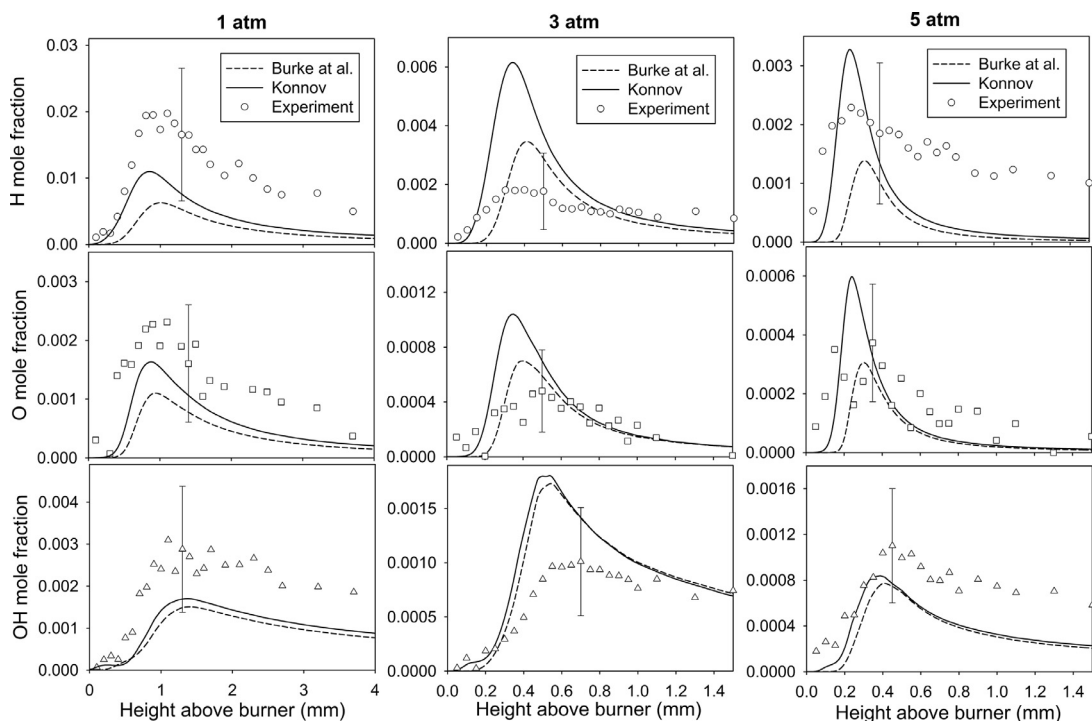


Fig. 3. Mole fraction profiles of H , O and OH in premixed laminar stoichiometric $\text{H}_2/\text{O}_2/\text{Ar}$ flames at pressures 1, 3 and 5 atm. Symbols: experimental data, lines: modeling.

mechanism of Burke et al. will be analyzed to interpret the observed pressure effects on the peak mole fractions of the flame species.

3.2. Pressure effect on the peak mole fractions of the flame intermediates

The pressure dependencies of peak mole fractions of H , O , OH , HO_2 radicals and H_2O_2 derived from the simulations using the Burke et al. mechanism are shown in Fig. 5. It should be remembered that the peaks for H , O , OH and HO_2 , H_2O_2 are located in different flame zones (see Figs. 3 and 4). As can be seen from Fig. 5, peak mole fractions of

H , and O radicals decrease with pressure. Although in the range from 1 to 3 atm mole fraction of OH practically does not change with pressure, its further increase to 5 atm results in a nearly twofold decrease in mole fraction of this radical. Moreover, the H/OH ratio decreases with pressure. Our previous study of methane flames in the same pressure range [19] showed similar tendencies: reduction of H and OH peak mole fractions and H/OH ratio with pressure. This was explained to be related primarily to the reaction $\text{H} + \text{O}_2 (+\text{M}) \leftrightarrow \text{HO}_2 (+\text{M})$, the contribution of which to H consumption increased with pressure. The rise in H/OH ratio was attributed, therefore, to enhanced production of

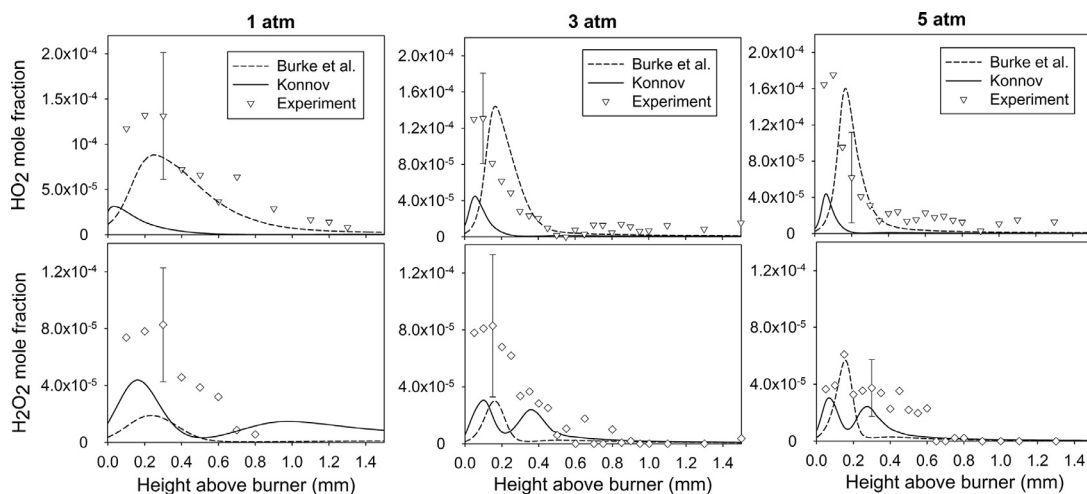


Fig. 4. Mole fraction profiles of HO_2 and H_2O_2 in premixed laminar stoichiometric $\text{H}_2/\text{O}_2/\text{Ar}$ flames at 1, 3 and 5 atm. Symbols: experimental data, lines: modeling.

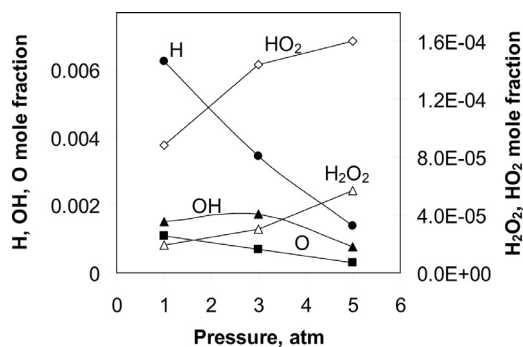


Fig. 5. Peak mole fractions of the flame intermediates, as derived from the calculations using the mechanism of Burke et al. [6].

HO_2 , which contributed to the formation of OH via the reactions of HO_2 with other flame radicals, like $\text{HO}_2 + \text{H} \rightleftharpoons \text{OH} + \text{OH}$. The kinetic analysis of the production and consumption routes of H and OH , according to the Burke et al. mechanism, showed that these arguments are also true for the hydrogen flame studied in this work to explain the observed trends for H and OH radicals.

To explain the reduction of O peak mole fraction with pressure (see Fig. 5), we performed an analysis of the reaction pathways responsible for production and consumption of O radicals in the flame (Fig. 6). Similarly as was done in our previous work [19], this analysis was carried out in terms of the contributions (in percents) of the integrated rate of each individual reaction to the total integrated rate of consumption of the selected species in the entire flame. An integrated reaction rate (mol/cm^3) was calculated in the same way as

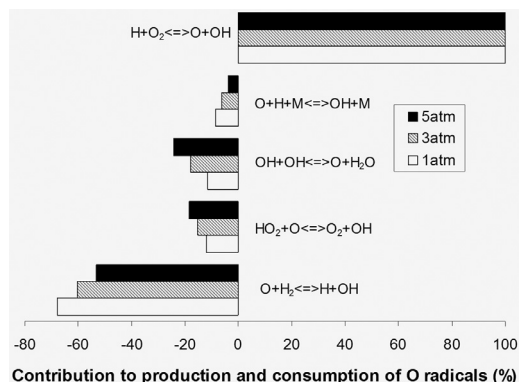


Fig. 6. Major contributions (in percents) of the integrated rates of the reactions to the total integrated rate of production and consumption of O radicals in stoichiometric $\text{H}_2/\text{O}_2/\text{Ar}$ flames at 1, 3 and 5 atm.

was proposed by Held and Dryer [30]:

$$\omega_i = \int_0^\infty \omega'_i dt = \int_0^\infty \frac{\omega'_i}{v} dx$$

where ω'_i is local rate of i th reaction, $\text{mol}/(\text{cm}^3\text{s})$, v is local gas velocity (cm/s), x is distance from the burner (integration is carried out over the entire flame zone). To calculate the total integrated rate of consumption of a selected species, the summation was performed over all possible reactions associated with consumption of the very species.

The reactions shown in Fig. 6 are written as they are in the kinetic mechanism, and they can proceed either in forward or reverse direction. As can be seen from Fig. 6, the chain branching re-

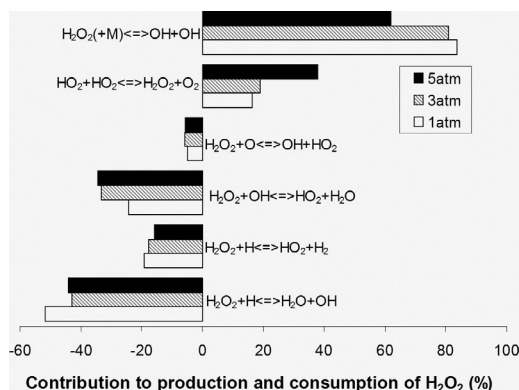


Fig. 7. Major contributions (in percents) of the integrated rates of the reactions to the total integrated rate of production and consumption of hydrogen peroxide in stoichiometric $\text{H}_2/\text{O}_2/\text{Ar}$ flames at 1, 3 and 5 atm.

action $\text{H} + \text{O}_2 = \text{O} + \text{OH}$ is the main source of O atoms in the flame, whereas another chain branching reaction ($\text{O} + \text{H}_2 = \text{H} + \text{OH}$) provides the main route for its consumption. The pressure rise results in a reduction of the contribution of the latter reaction to O consumption. However, meanwhile the reactions of O with HO_2 ($\text{O} + \text{HO}_2 = \text{O}_2 + \text{OH}$) and water ($\text{O} + \text{H}_2\text{O} = \text{OH} + \text{OH}$) yielding OH radicals provide more significant contribution to consumption of O atoms with pressure. These reactions are likely to be responsible for reduction of the peak mole fraction of O radicals with pressure.

Further discussion will be focused on the kinetics of peroxy species in the flame. The increase in HO_2 peak mole fraction with pressure (see Fig. 5) is a result of the competition between the dominant reaction of its formation $\text{H} + \text{O}_2 (+\text{M}) \leftrightarrow \text{HO}_2 (+\text{M})$ (R1), the rate constant of which is pressure-dependent, and the main reaction of its consumption $\text{HO}_2 + \text{H} \leftrightarrow \text{OH} + \text{OH}$ (R2). Although the maximums of the rates of these reactions are located at different temperatures, the ratio of maximum rate of the reaction R1 to the maximum rate of the reaction R2 was found to increase with pressure as 1.32, 1.45 and 1.56 for 1, 3, and 5 atm, respectively. Hence, this leads to an enhanced HO_2 formation with pressure.

To interpret the increase of H_2O_2 peak mole fraction with pressure (Fig. 5) we calculated the contributions of reaction pathways responsible for its production and consumption (Fig. 7). These calculations were made similarly as described above for O radicals. As can be seen from Fig. 7, there are two routes of H_2O_2 production: via recombination of two OH radicals ($\text{OH} + \text{OH} = \text{H}_2\text{O}_2(+\text{M})$) or HO_2 radicals ($\text{HO}_2 + \text{HO}_2 = \text{H}_2\text{O}_2 + \text{O}_2$). The reactions of H_2O_2 with H ($\text{H}_2\text{O}_2 + \text{H} = \text{H}_2\text{O} + \text{OH}$ and $\text{H}_2\text{O}_2 + \text{H} = \text{HO}_2 + \text{H}_2$), OH ($\text{H}_2\text{O}_2 + \text{OH} = \text{HO}_2$

+ H_2O) and O ($\text{H}_2\text{O}_2 + \text{O} = \text{OH} + \text{HO}_2$) provide its consumption. Despite the fact that the contributions of all these reactions change with pressure, the contribution of the reaction of HO_2 recombination becomes particularly significant when pressure rises from 3 to 5 atm. Therefore, the increase in the peak mole fraction of hydrogen peroxide can be attributed to the increased role of the reaction $\text{HO}_2 + \text{HO}_2 = \text{H}_2\text{O}_2 + \text{O}_2$.

Summarizing the findings represented above, we come, thus, to a conclusion that the reactions involving peroxy radicals play an important role in the combustion process of hydrogen at least in the pressure range 1–5 atm. Although this fact was already discussed earlier in the literature, see e.g., [8], the corresponding conclusions were based on the kinetic models which were not validated against detailed speciation measurements in the flames at the pressures higher than atmospheric. The experimental data represented in this work provided this basis. Furthermore, these data can be used for further development and improvement of future kinetic models of hydrogen combustion at elevated pressures.

4. Conclusions

In this work, the mole fraction profiles of the major stable species (H_2 , O_2 , H_2O) and all intermediates including H, O, OH, HO_2 , and H_2O_2 were measured by a flame-sampling molecular-beam mass spectrometric technique in laminar stoichiometric premixed burner-stabilized $\text{H}_2/\text{O}_2/\text{Ar}$ flames at pressures of 1–5 atm. The experimental data were compared with the results of numerical simulations using two detailed chemical kinetic mechanisms recently developed for hydrogen combustion by Konnov [5] and Burke et al [6]. The simulations were performed using the temperature profiles measured with thermocouples in the presence of the sampling probe to take into account the flame cooling effect by the probe. Both mechanisms adequately reproduced the mole fraction profiles of the major components and H, O, OH radicals in the flame at the pressures considered. However, the mechanism of Burke et al. was found to be more accurate in predicting mole fraction profiles of peroxy species (HO_2 and H_2O_2) in the flames. The observed reduction in the peak mole fractions of H, O, OH radicals and increase in the peak mole fractions of HO_2 and H_2O_2 with pressure was explained basing on the results of a kinetic analysis of the Burke et al. model. The experimental results represented in this work provide a complete survey of the structure of the burner-stabilized premixed flame of hydrogen in the pressure range from 1 to 5 atm and can help to improve future kinetic models of hydrogen combustion.

Acknowledgments

This work was supported financially by the Ministry of Education and Science of Russian Federation (project 14.Y26.31.0003).

Supplementary materials

Supplementary material associated with this article can be found, in the online version, at doi:10.1016/j.proci.2016.07.109.

References

- [1] J. Li, Z. Zhao, A. Kazakov, M. Chaos, F.L. Dryer, J.J. Scire Jr., *Int. J. Chem. Kinet.* 39 (2007) 109–136.
- [2] H. Wang, X. You, A.V. Joshi, S.G. Davis, A. Laskin, F. Egolfopoulos, C.K. Law, USC Mech Version II. High Temperature Combustion Reaction Model of H₂/CO/CI-C₄ Compound, May 2007, http://ignis.usc.edu/USC_Mech_II.htm
- [3] M. O’Connaire, H.J. Curran, J.M. Simmie, W.J. Pitz, C.K. Westbrook, *Int. J. Chem. Kinet.* 36 (2004) 603–622.
- [4] S.C. Davis, A.V. Joshi, H. Wang, F. Egolfopoulos, *Proc. Combust. Inst.* 30 (2005) 1283–1292.
- [5] A.A. Konnov, *Combust. Flame* 152 (2008) 507–528.
- [6] M.P. Burke, M. Chaos, Y. Ju, F.L. Dryer, S.J. Klippenstein, *Int. J. Chem. Kinet.* 44 (2012) 444–474.
- [7] V.A. Alekseev, M. Christensen, E. Berrocal, E.J.K. Nilsson, A.A. Konnov, *Combust. Flame* 162 (10) (2015) 4063–4074.
- [8] A.L. Sánchez, F.A. Williams, *Prog. Energy Combust. Sci.* 41 (2014) 1–55.
- [9] K.N. Bascombe, *Proc. Combust. Inst.* 10 (1965) 55–64.
- [10] G. Dixon-Lewis, M.M. Sutton, A. Williams, *Proc. Combust. Inst.* 10 (1965) 495–502.
- [11] K.H. Eberius, K. Hoyermann, G.G. Wagner, *Proc. Combust. Inst.* 13 (1971) 713–721.
- [12] G. Dixon-Lewis, M.M. Sutton, A. Williams, *Proc. R. Soc. Lond. A* 317 (1970) 227–234.
- [13] N.J. Brown, K.H. Eberius, R.M. Fristrom, K. Hoyermann, G.G. Wagner, *Combust. Flame* 33 (1978) 151–160.
- [14] K. Kohse-Höinghaus, P. Koczar, Th. Just, *Proc. Combust. Inst.* 21 (1986) 1719–1727.
- [15] J. Vandoooren, J. Bian, *Proc. Combust. Inst.* 23 (1990) 341–346.
- [16] A.A. Paletskii, L.V. Kuibida, T.A. Bolshova, O.P. Korobeinichev, R.M. Fristrom, *Combust. Explos. Shock Waves* 32 (1996) 245–250.
- [17] O.P. Korobeinichev, V.M. Shvartsberg, S.B. Il’in, A.A. Chernov, T.A. Bol’shova, *Combust. Explos. Shock Waves* 35 (1999) 239–244.
- [18] A.G. Shmakov, O.P. Korobeinichev, I.V. Rybitskaya, A.A. Chernov, D.A. Knyazkov, T.A. Bolshova, A.A. Konnov, *Combust. Flame* 157 (2010) 556–565.
- [19] A.M. Dmitriev, D.A. Knyazkov, T.A. Bolshova, A.G. Tereshchenko, A.A. Paletsky, A.G. Shmakov, O.P. Korobeinichev, *Combust. Flame* 162 (2015) 3946–3959.
- [20] O.P. Korobeinichev, S.B. Ilyin, V.M. Shvartsberg, A.A. Chernov, *Combust. Flame* 118 (1999) 718–726.
- [21] S.N. Foner, R.L. Hudson, *J. Chem. Phys.* 36 (1962) 2681.
- [22] C.J. Aul, M.W. Crofton, J.D. Mertens, E.L. Petersen, *Proc. Combust. Inst.* 33 (2011) 709–716.
- [23] T.A. Cool, K. Nakajima, K.A. Taatjes, A. McIlroy, P.R. Westmoreland, M.E. Law, A. Morel, *Proc. Combust. Inst.* 30 (2005) 1681–1688.
- [24] Y.-K. Kim, K.K. Irikura, M.E. Rudd, M.A. Ali, P.M. Stone, J. Chang, J.S. Coursey, R.A. Dragoset, A.R. Kishore, K.J. Olsen, A.M. Sansonetti, G.G. Wiersma, D.S. Zucker, M.A. Zucker, available at <http://physics.nist.gov/PhysRefData/Ionization>.
- [25] K.N. Josphipura, M. Vinodkumar, U.M. Patel, *J. Phys. B: At. Mol. Opt. Phys.* 34 (2001) 509–519.
- [26] R.J. Kee, J.F. Grcar, M.D. Smooke, J.A. Miller, *PREMIX: A Fortran Program for Modeling Steady Laminar One-Dimensional Premixed Flames*, Report No. SAND85-8240 Sandia National Laboratories, Livermore CA, 1993.
- [27] A.N. Hayhurst, N.R. Telford, *Proc. Roy. Soc. Lond., Ser. A* 322 (1971) 483–507.
- [28] A.N. Hayhurst, *Combust. Explos. Shock Waves* 48 (5) (2012) 516–525.
- [29] C.R. Shaddix, in: Proceedings of the 33rd National Heat Transfer Conference, Albuquerque, New Mexico, ASME, New York, 1999 Paper HTD99-282.
- [30] T.J. Held, F.L. Dryer, *Int. J. Chem. Kin.* 30 (11) (1998) 805–830.